JACS
JOURNAL OF THE AMERICAN CHEMICAL SOCIETY
Article
pubs.acs.org/JACS

Bond-Making and Breaking between Carbon, Nitrogen, and Oxygen in Electrocatalysis

Hongjiao Li,[†,‡] Yongdan Li,[‡] Marc T. M. Koper,*[,†] and Federico Calle-Vallejo*[,§]

[†]Leiden Institute of Chemistry, Leiden University, 2300 RA, Leiden, The Netherlands

[‡]Tianjin Key Laboratory of Applied Catalysis Science and Technology and State Key Laboratory for Chemical Engineering, School of Chemical Engineering and Technology, Tianjin University, Tianjin 300072, People's Republic of China

[§]Laboratoire de Chimie, ENS Lyon, Université de Lyon, CNRS, 46 allée d'Italie, 69364 Lyon Cedex 07, France

Supporting Information

ABSTRACT: Many catalytic reactions involving small molecules, which are key transformations in sustainable energy and chemistry, involve the making or breaking of a bond between carbon, nitrogen and oxygen. It has been observed that such heterogeneously (electro)catalyzed reactions often exhibit remarkable and unusual structure sensitivity, in the sense that they take place preferentially on catalyst surfaces with a long-ranged two-dimensional (100) atomic structure. Steps and defects in this two-dimensional structure *lower* the catalytic activity. Such structure sensitivity must be due to the existence of a special active site on these two-dimensional (100) terraces. Employing detailed density functional theory calculations, we report here the identification of this special active site for a variety of catalytic reactions. The calculations also illustrate how this specific site breaks the well-known rule that under-coordinated surface atoms bind adsorbates stronger, thereby providing the atomic-level explanation for the lack of reactivity of steps and defects for the reactions under consideration. The breakdown of such rule results in significant deviations from commonly observed energetic scaling relations between chemisorbates. Thus, this work provides new design rules for the development of thermodynamically efficient catalysts for an important class of bond-making and bond-breaking reactions.

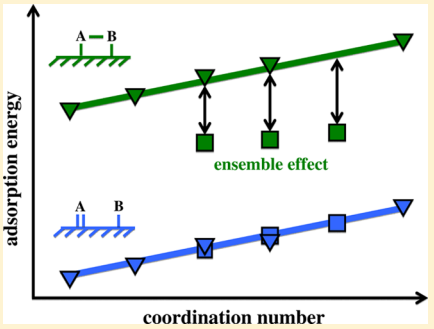

1. INTRODUCTION

Heterogeneously catalyzed reactions are often highly sensitive to the exact atomic structure of the catalyst surface. This phenomenon is known as structure sensitivity and is normally studied experimentally by using well-defined single-crystal catalyst surfaces, or by using tailor-made shape-controlled nanoparticles.[1,2] It has been recently noted that in electrocatalysis, there is a prominent class of reactions that takes place preferentially on two-dimensional terraces of (100) orientation, and that these reactions always involve the breaking or making of a bond between carbon, nitrogen and oxygen.[2] These reactions include the electrochemical oxidation of ammonia on platinum,[3,4] the oxidation of dimethyl ether on platinum,[5−7] the reduction of nitrite on platinum,[8] the reduction of carbon monoxide to ethylene on copper,[9,10] and the reduction of oxygen on a gold electrode.[11−13] Presumably, there are more, yet to be discovered examples. Steps or defects in the two-dimensional nature of the (100) electrocatalyst surface have a strong detrimental effect on the activity of these reactions. This is an unusual and counterintuitive observation, as typically it is believed that steps and defects in a surface act as active sites for catalysis. There are also some examples of such structure sensitivity in surface science studies of heterogeneous catalysis,[14] but the phenomenon seems less well documented than in electrocatalysis.

In a recent paper, the structure sensitive oxidation of dimethyl ether ($H_3C-O-CH_3$) to carbon dioxide on platinum single-crystal electrodes in acidic media was studied.[5] Since the work of Ye et al.,[6,7] this reaction, which is of potential interest to low-temperature fuel cells, has been known to take place preferentially on Pt(100) terraces. It was confirmed experimentally that steps in the (100) terrace indeed inhibit the C−O bond breaking, lowering the overall oxidation activity. From detailed density functional theory (DFT) calculations, we concluded that the critical bond-breaking step occurs in a *HCOC intermediate bound to a square arrangement of four platinum surface atoms in the (100) terrace. Optimization of the number of active surface sites then automatically requires large two-dimensional (100) terraces. In terms of practical catalysis, it implies that the optimal nanoparticle catalyst must have a cubical shape or at least present a large fraction of two-dimensional (100) facets.[15−17] In this paper, we will generalize these findings to a number of other reactions, and will elucidate why the square arrangement of surface atoms is such a good bond-making and bond-breaking site by showing how it violates the general rule in surface chemistry that atoms with low coordination numbers provide stronger chemisorption properties.[18] This rule stems from the fact that the geometric and

Received: August 22, 2014
Published: October 14, 2014

dx.doi.org/10.1021/ja508649p | J. Am. Chem. Soc. 2014, 136, 15694−15701

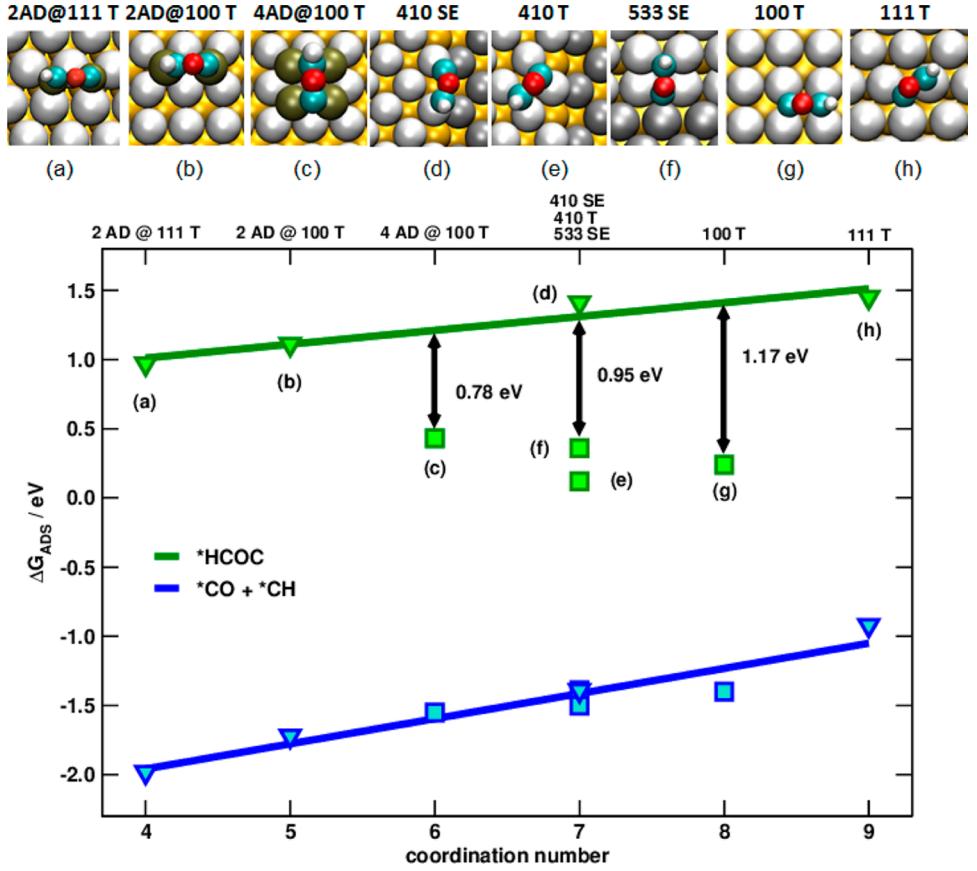

Figure 1. Evolution of the adsorption energies of *HCOC (green) and *CO + *CH (blue) according to the coordination number of the active sites on platinum (the upper *x*-axis enumerates the facets, where T stands for terrace, SE for step edge and AD for platinum adatoms). Sites with/without ensemble effects are represented by squares/triangles. Images of *HCOC on the different sites and facets are shown in (a–h). The yellow, large white and gray, and dark green atoms are bulk, surface, and adatoms of platinum, while the blue, red and small white atoms are carbon, oxygen and hydrogen atoms, respectively.

electronic structures of metals are closely connected, such that band centers and widths are found to be directly proportional to coordination numbers.[18−20] We will also show that the violation of such rule results in large departures from scaling relations,[21,22] which can enable the design of more thermodynamically efficient catalysts. Considering the great importance of C−C, C−O, C−N, N−O, N−N, and O−O bond-making and breaking reactions in (electro)catalysis, this insight provides a fundamental and hitherto unrecognized rule for optimal catalyst design. For the remainder of the paper, we will often refer to the special active site as an "ensemble" site, where we define an ensemble as a specific arrangement of surface atoms that favors a certain reaction. This definition does not include the frequency of occurrence of the site; in fact, the ensemble site considered in this paper occurs naturally and with very high density on (100) terraces.

In the following, we will present DFT calculations for four reactions that have been shown experimentally to exhibit this special structure sensitivity for (100) terraces: dimethyl ether oxidation on platinum, carbon monoxide reduction on copper, ammonia oxidation on platinum, and oxygen reduction on gold. For these four reactions, we will identify the catalytically active site on the (100) surface as well as a remarkable commonality in terms of structure sensitivity.

2. RESULTS AND DISCUSSION

2.1. Dimethyl Ether Oxidation on Platinum. The overall redox reaction for the oxidation of dimethyl ether (DME) is

$$CH_3OCH_3 + 3H_2O \rightarrow 2CO_2 + 12(H^+ + e^-) \quad (1)$$

By combining experimental and computational data, we have established that on platinum the most likely mechanism for this reaction follows an initial series of dehydrogenation steps to the adsorbed *HCOC stage[5] (the * henceforth denoting a chemisorbed species). The C−O bond then breaks and the resulting chemisorbed *CO and *CH fragments are oxidized to CO_2. The *HCOC species was identified as the species in which the C−O bond breaks based on DFT calculations showing that it is the most stable species on Pt(100) in the potential window of interest, and because it has the highest driving force and lowest activation energy toward bond breaking among the various *H_xCOC adsorbates. The *HCOC species is much more stable on Pt(100) than on Pt(111) because of the particular "double-bridged" state in which it binds to the Pt(100) (see Figure 1g). This adsorption state explains the unique activity of Pt(100) for reaction 1.

We show here that whenever this particular binding geometry of two opposing bridge sites is available on the Pt surface, *HCOC exhibits strong binding, in stark contrast to species that bind with only the C atom to the surface, such as *CH and *CO. In Figure 1 we plot the free energies of adsorption of *HCOC species and the combined adsorption

dx.doi.org/10.1021/ja508649p | J. Am. Chem. Soc. 2014, 136, 15694−15701

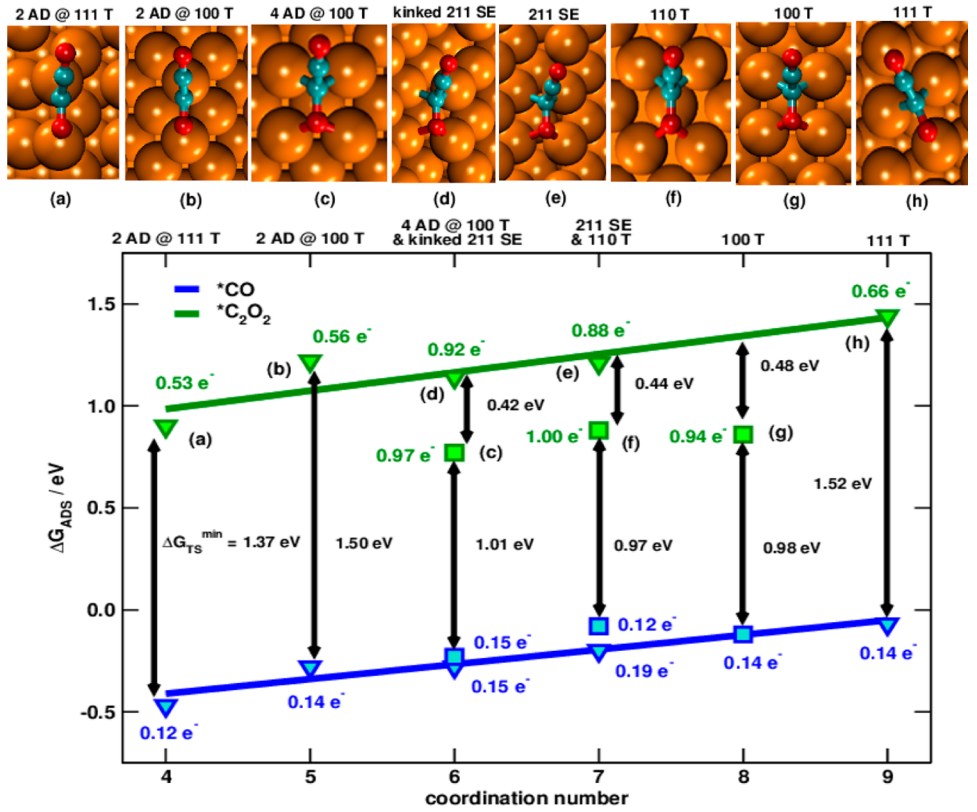

Figure 2. Evolution of the adsorption energies of *CO (blue) and $*C_2O_2$ (green) according to the coordination number of the active sites on copper (the upper *x*-axis enumerates the facets, where T stands for terrace, SE for step edge and AD for copper adatoms). Sites with/without ensemble effects are represented by squares/triangles. The numbers in black correspond to the minimum barriers for the transformation of two CO moieties into $*C_2O_2$. No solvation was included in the computation of the adsorption energies.

energy of (isolated) *CO and *CH for a number of different surfaces (details of the DFT calculations, the estimation of free energies, and the most stable adsorption geometries are given in the Supporting Information). The surfaces have been ordered along the abscissa according to the increasing coordination number of the surface atoms in the site under consideration. It is expected that adsorbates such as *CO and *CH exhibit a stronger binding to a Pt surface site with a lower surface coordination, and this trend is indeed confirmed by the DFT calculations (blue data points in Figure 1). However, for *HCOC this rule is violated whenever the (100)-type double-bridged coordination site is available on the surface, as this "ensemble" provides a particularly stable adsorption geometry (green-square data points in Figure 1). No such special adsorption geometry exists for the $*H_2COC$ adsorbate for instance, and therefore the $*H_2COC$ follows the rule that a lower surface atom coordination leads to stronger binding (as illustrated in Figure S1).

The analysis illustrated in Figure 1 explains why large (100) terraces are needed for this reaction, as in that way the number of ensemble sites is maximized. Steps and defects break this two-dimensional lattice of ensemble sites. Note that the step sites in the Pt(533) surface are also predicted to be active, but clearly the Pt(533) should be much less active than Pt(100). This prediction has been verified experimentally as shown in Figure S3 in the Supporting Information. The above analysis also confirms that *HCOC is indeed the most likely key intermediate for DME oxidation.

2.2. Carbon Monoxide Reduction on Copper. Copper surfaces are unique electrocatalysts for the reduction of CO_2 and CO in aqueous media, as was first shown by Hori in the 1980s.[23,24] One of the most surprising observations in this reaction, which is currently regaining much attention, is the formation of significant amounts of C_2 products, especially ethylene, from CO (and also from CO_2), through the following redox reaction:

$$2CO + 8(H^+ + e^-) \rightarrow C_2H_4 + 2H_2O \quad (2)$$

We showed recently that Cu(100) is particularly active for the reduction of CO to C_2H_4, and that steps in the Cu(100) surface lower the activity toward this reaction.[9,10] From DFT calculations, we concluded that a chemisorbed CO dimer (i.e., C_2O_2) is the key intermediate in the C−C bond formation step on Cu(100).[25] In addition, the existence of this intermediate, which is formed by electron transfer rather than by proton-coupled electron transfer, naturally explains the pH dependence of the ethylene formation from CO (for details see refs[10,25−28]).

To evince the unique ability of square sites of Cu to reduce CO to C_2H_4 we show in Figure 2 the adsorption energies of the species involved in the rate-limiting step, i.e., *CO and $*C_2O_2$, as a function of the coordination number of the active sites. The trends in *CO adsorption are approximately linear; i.e., the lower the surface coordination of the active site, the stronger the *CO binding energies. This effect is largely independent of the actual geometry of the surface, since sites with the same coordination number have similar *CO adsorption energies. The trends in $*C_2O_2$ are somewhat similar, but deviations from the trend are observed whenever the dimer binds to a surface site with a square (or rectangular) symmetry. This geometry lowers the adsorption energy by as much as 0.4−0.5 eV.

dx.doi.org/10.1021/ja508649p | J. Am. Chem. Soc. 2014, 136, 15694−15701

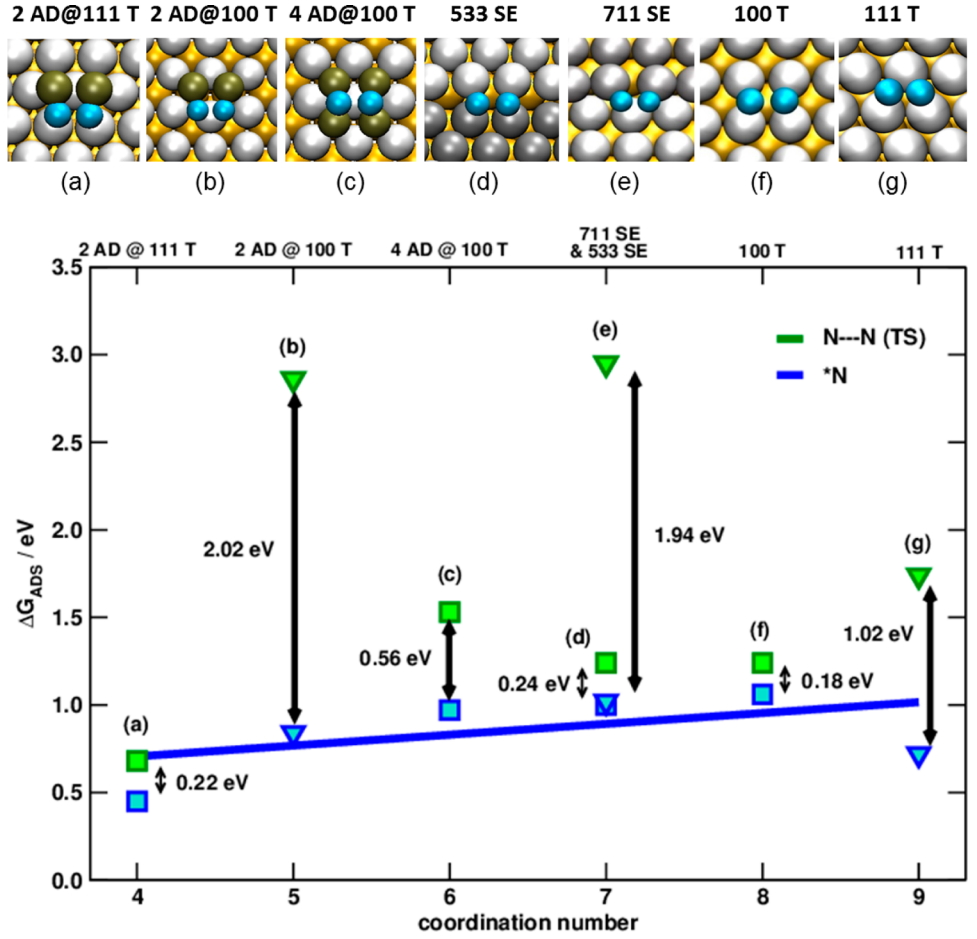

Figure 3. Adsorption energies of *N (blue) and of the $*N_2^{\#}$ transition state (green) as a function of the coordination number of the active sites on different platinum surfaces (the upper *x*-axis lists the facets, where T stands for terrace, SE for step edge and AD for platinum adatom). Sites with/without ensemble effects are represented by squares/triangles. Images of TS on the different sites and facets are shown in (a–g).

Therefore, $*C_2O_2$ is a geometry-sensitive adsorbate that strongly prefers square-symmetry surface sites. As a result, sites with identical coordination environments but different geometries exhibit dissimilar adsorption properties.

The observation of an ensemble effect for $*C_2O_2$ adsorption and not for *CO, leads to a distinction between the catalytic activity of sites with hexagonal and square symmetry. Since the coupling of CO moieties results in the formation of $*C_2O_2$ and this reaction is uphill, the lowest possible kinetic barrier is given by the difference in adsorption energies of both adsorbates, which corresponds to the black vertical lines in Figure 2. Clearly, sites with square symmetry display barriers that are at least 0.4 eV lower than those with hexagonal symmetry.

In Figure 2 we have also indicated the excess electronic charges on the adsorbates, calculated through Bader's method.[29] The average excess charge on *CO is only 0.15 electrons. This indicates that although *CO is a strongly bound species, its adsorption is not accompanied by significant net charge transfer between adsorbates and surface sites. On the other hand, the adsorption of $*C_2O_2$ is mediated by a large charge transfer from the surface to the adsorbate, the amount of which is maximum at sites with square symmetry. For these sites, the charge transfer is on the order of 1 electron, which shows that the dimer is negatively charged in its adsorbed state. This feature explains why ethylene formation from CO on Cu(100) is pH independent, as the rate-limiting step is an electron-mediated coupling of two CO moieties in which no protons are involved. Generally speaking, the ensemble effect in CO reduction to ethylene on Cu electrocatalysts is geometric in the sense that only square-like sites allow for suitable adsorption configurations with low kinetic barriers, and is also electronic, as the charge donated by the surface to facilitate the C–C coupling is larger at sites formed by four atoms, compared to hexagonal-symmetry sites formed by three atoms. The calculations were performed in the absence of water but it may be expected that its presence will have a further stabilizing effect on the charged intermediates. We note that in aprotic solvents such as ammonia, CO electroreduction leads to the formation of a negatively charged dimer as the only product, proving the natural tendency of CO to dimerize under electron-donating conditions.[27]

2.3. Ammonia Oxidation on Platinum. The electrocatalytic oxidation of ammonia (NH_3) to dinitrogen (N_2) on platinum single-crystal electrodes is the prototypical example of a structure-sensitive reaction preferring two-dimensional Pt(100) terraces.[3,4] Nitrogen is observed to evolve from a potential of ca. 0.5 V_{RHE} on a Pt(100) electrode, and the introduction of steps leads to a substantial lowering of the N_2 formation current. The relevant intermediate(s) leading to the N–N bond formation during electrochemical ammonia oxidation have been under debate since the 1970s (for a review, see[30]). On Pt(100), DFT calculations show that the most stable ammonia intermediate is $*NH_2$. Rosca and Koper have suggested that two $*NH_2$ may dimerize to surface-

dx.doi.org/10.1021/ja508649p | J. Am. Chem. Soc. 2014, 136, 15694–15701

adsorbed hydrazine (N_2H_4),[31] but DFT calculations show that this reaction has a very high barrier (see Supporting Information). The formation of *NH is thermodynamically unfavorable, and would not take place before ca. 0.9 V_{RHE}, if the coadsorption of water or *OH is not taken into account. However, in the presence of coadsorbed *OH, which exists on the Pt(100) electrode in the relevant potential window, *NH is relatively more stable on Pt(100) than *NH_2. Our DFT calculations suggest that at high coverage *NH and *OH do not repel each other as much as *NH_2 and *OH do, shifting the formation potential of *NH to ca. 0.69 V_{RHE}. At this potential, *N is predicted to be thermodynamically more stable than *NH, though there may be a barrier for its formation. Therefore, the actual N−N bond formation follows either from the dimerization of two *NH or two *N moieties. Ishikawa et al.[32] have recently studied the energetics of both reactions and suggest that the dimerization of *N on the Pt(100) surface is the more likely step leading to the formation of N_2.

We follow here the suggestion by Ishikawa et al. that the N−N bond is formed from the reaction between two *N. Interestingly, for this reaction we find that the initial state (i.e., 2 *N) and the final state (weakly adsorbed *N_2) do not always prefer the double-bridge ensemble site, but the transition state does. Figure 3 plots the binding energy of 2*N in the initial state (blue line) and the energy of the *$N_2^{\#}$ transition state vs the coordination number of surface atoms to which the intermediates bind on the various surfaces. Atomic nitrogen always prefers a 3- or 4-fold coordination to the surface, and binds strongest to the Pt(111) surface (an observation made before,[33] which deviates from the coordination rule[18]). More importantly, the transition state corresponding to the recombination of 2 *N always has the lowest energy over a double-bridge ensemble site, as illustrated by the green-square data points in Figure 3. Transition states in which the nitrogen atoms cannot bind to two opposing bridge sites have a significantly higher energy. A very similar conclusion is drawn from an analysis of the 2*NH → *N_2H_2 reaction (see Supporting Information Figure S11), where either the initial or the final state may not prefer the double-bridge ensemble site, but the transition state always does. However, the corresponding activation energy is always higher than for the 2*N → N_2 reaction, and since *N also appears to be more thermodynamically stable, at least on Pt(100), the latter reaction is the more likely N−N bond forming reaction.

2.4. Oxygen Reduction on Au. The electrocatalytic reduction of oxygen on gold single-crystal electrodes is the final example of the special structure sensitivity under consideration in this paper. Adzic et al. have shown that Au(100) is the most active surface for the 4-electron transfer reduction to water in alkaline media.[12] Steps in the Au(100) surface lower the activity for the 4-electron reduction, whereas the other two low-index surfaces (i.e., Au(111) and Au(110)) can only perform the two-electron transfer reduction to peroxide HO_2^-. Steps of (100) orientation have a higher activity than (111) terraces, but the optimal 4-electron transfer activity is always observed for electrodes with large (100) terraces.[13]

The mechanism for oxygen reduction on gold is different from the mechanism typically considered for platinum. One important difference is the strong pH dependence: gold shows its highest activity in alkaline media. This is explained by the first step being an electron transfer step without simultaneous proton transfer, followed by the formation of an (adsorbed) peroxide intermediate (for a detailed discussion, see ref.[34]):

$$O_2 + e^- \rightarrow O_2^- \quad (3)$$

$$O_2^- + H^+ + e^- \rightarrow HO_2^- \quad (4)$$

where O_2^- and HO_2^- may or may not be (weakly) adsorbed on the gold surface. The stability or adsorption energy of the peroxide intermediate is a good indicator of the ORR activity.[35] It may diffuse away from the electrode surface, or it may bind to the surface as *OOH and dissociate into *O + *OH, thereby determining the bifurcation between 2- and 4-electron reaction pathways. The *O and *OH adsorbates are archetypal ORR intermediates,[36,37] as their reduction produces H_2O (OH^- in alkaline media), thereby concluding the 4-electron reduction of O_2.

In Figure 4a we plot the computed free energies corresponding to the equilibrium potentials of the redox transformations of O_2 to H_2O and H_2O_2 (black and red horizontal lines at −1.23 and −0.68 eV, respectively), together with the free energies of *OH and *OOH in the scales relevant to reduce oxygen: *OOH formed from O_2, and *OH forming H_2O. The way to read Figure 4a is to realize that in order to reduce O_2 to H_2O and avoid H_2O_2 formation, the free reaction energies for both reaction steps involving *OH and *OOH should be more negative than the standard free energy of H_2O_2 formation, set at −0.68 eV. This condition is satisfied only by Au(100) due to the ensemble effect that stabilizes *OOH and moves it apart from the expected trend by ca. 0.30 eV. Figure 4a also predicts that (100) step edges in Au(211), which have square symmetry, may have the ability to produce H_2O, in agreement with experimental observations showing that square-like steps are active for the 4-electron reduction of oxygen but display much lower activities than pristine Au(100).[11,13]

As a second argument for the special reactivity of the Au(100) surface for the ORR, we note that since Au(100) is also the only surface that is able to reduce HO_2^- to water (in alkaline media[38]), it is reasonable to assume that the O−O bond breaking occurs in this intermediate. In Figure 4b, we plot the binding energy of *OOH and the binding energy of coadsorbed *O + *OH as a function of the surface coordination of the gold surface sites. It is observed that binding sites with square (100) geometry provide an especially strong binding for the coadsorbed *O + *OH fragments, leading to a stronger driving force for bond breaking. Figure S12 in the Supporting Information compares the potential energy profiles for *OOH bond breaking into *O + *OH on Au(111) and Au(100). On Au(111), the separation of the *O and *OH fragments leads to a lowering of the free energy of ca. 0.05 eV (see Table S8 in the Supporting Information for details of the magnitude and origin of this effect on the different Au facets). On the other hand, on the Au(100) surface the coadsorbed state is lower in energy than the separate states by 0.22 eV, due to the favorable hydrogen-bond interaction between *O and *OH (see the rightmost image in Figure S12). This stabilization occurs only in the (100) double-bridge ensemble site, and leads to the large driving force for O−O bond breaking. On Au(100) the activation energy for the O−O bond breaking is also lower by 0.24 eV compared to that on Au(111) .

In summary, the 4-electron reduction of oxygen on Au(100) is enabled by the sizable stabilization of the *OOH intermediate on this surface, in conjunction with the facilitated

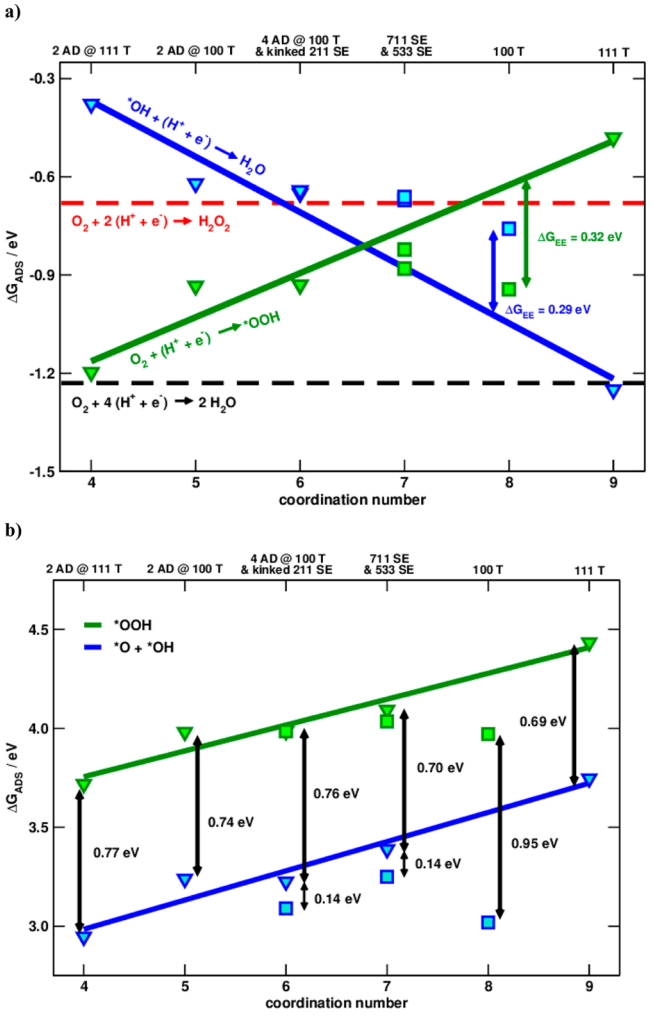

Figure 4. (a) Trends in the energetics of O_2 protonation to produce *OOH (green) and *OH protonation to produce H_2O (blue) as described by the coordination numbers of the active sites. ΔG_{EE} is the adsorption energy gained by *OOH and *OH species due to the presence of the 4-atom ensemble effect in pristine (100) terraces. (b) Evolution of the adsorption energies of *OH + *O (blue) and *OOH (green) according to the coordination number of the active sites on gold (the upper *x*-axis enumerates in both cases the facets, where T stands for terrace, SE for step edge and AD for gold adatoms). Sites with/without ensemble effects are represented by squares/triangles. Images of the coadsorption of *OH + *O on different facets are shown in Figure S13.

breaking of the O−O bond by the enhanced thermodynamic driving force and reduced kinetic barrier compared to other facets.

3. GENERAL DISCUSSION

In the previous sections, we have described how (100) surfaces and surfaces with (100) sites show a special reactivity for the making and breaking of bonds between carbon, nitrogen and oxygen, on the examples of the electrocatalytic dimethyl ether oxidation on Pt, carbon monoxide reduction on Cu, ammonia oxidation on Pt, and oxygen reduction on Au. This special reactivity is related to the double-bridge ensemble site, which is found to be poised specifically for bond making and bond breaking. The ensemble site can promote bond making or bond breaking for essentially three reasons:

(1) The precursor(s) to bond making or bond breaking prefers to bind to this ensemble site. The bonding of the *HCOC intermediate during dimethyl ether oxidation on Pt(100) is a specific example. Also the specific stabilization of *OOH on Au(100) sites plays a role in the high reactivity of this surface for oxygen reduction.

(2) The product(s) of bond making or bond breaking prefers to bind to this ensemble site. The bonding of the $*C_2O_2$ intermediate during the reduction of CO on Cu(100) is a good example of this effect. Also the specific stabilization experienced by the coadsorption of *O and *OH on the ensemble site aids in lowering the activation energy for bond breaking in the *OOH intermediate during oxygen reduction on Au. Typically, this kind of stabilization leads to a lower activation energy for bond breaking or bond making owing to the Brønsted−Evans−Polanyi relation between activation energy and thermodynamic driving force.[39,40]

(3) The activation energy for bond making or bond breaking is the lowest in this ensemble site, or in other words, the relevant transition state is stabilized in the ensemble site. The specific example given above is the transition state for N−N bond formation from two *N adsorbates on Pt(100).

We have also illustrated how the double-bridge ensemble site provides stabilization to the key intermediate for bond making or bond breaking in a way that does not follow the usual rule that a more open surface with low-coordinated surface atoms provides a stronger binding.[18] This is primarily because the intermediate or the transition state needs to bind to the surface in a bridged manner, and such coordination is most favorable when the bridging is between two opposing bridge sites, as offered by the double-bridge ensemble site. The preferential binding of *OOH to Au(100) may be an exception, as the stabilization of this intermediate appears to be more of an electronic than a geometrical origin. Since the (100) terrace provides the highest density of double-bridge ensemble sites, this surface is always the most active for reactions in which the making or breaking of bonds is rate determining. Steps in the (100) surface lower the overall activity as they do not provide the necessary ensemble site. Surfaces with isolated (100) sites will still show some activity, but the activity is never as high as for the perfect defect-free (100) terrace.

It is important to emphasize that not every reaction in which a bond between carbon, nitrogen and/or oxygen is made or broken will preferentially take place on a (100) surface. This depends on whether the bond-making or bond-breaking step is rate determining. If the bond-making or bond-breaking step is "fast enough" on other sites or facets, and the kinetic or thermodynamic bottleneck in a mechanism lies in another step of the mechanism, there is no expectation that the reaction will prefer the (100) surface for the reasons outlined in this paper. For instance, the oxygen reduction to water on a platinum electrode has no specific preference for the Pt(100) surface, as the O−O bond-breaking step (presumably in the *OOH intermediate) on platinum is not involved in the rate-determining step and is sufficiently fast on the Pt(111) facet. Therefore, the optimal site for the overall reaction depends on a combination of electronic and geometric factors. However, we do believe that if the bond-making or bond-breaking between C, N, O is rate determining, there are very good reasons to assume that the (100) facet will provide the highest overall reaction rate. A second important point to stress is that this rule applies to bonds between C, N, and O. These usually "fit" well geometrically to the double-bridge ensemble site. Bonds

dx.doi.org/10.1021/ja508649p | J. Am. Chem. Soc. 2014, 136, 15694−15701

between C or O and H, i.e., C−H and O−H, do not break preferentially over the site considered here. As Van Santen[41] has pointed out, such bonds preferentially break or form over single atoms, and therefore reactions in which the breaking or making of an O−H or C−H bond is the kinetic or thermodynamic bottleneck, often prefer undercoordinated stepped sites. This also agrees well with some of the structure sensitivity trends observed in experimental electrocatalysis.[2]

Summarizing, the trends shown in Figures 1−3 and 4b are useful to show the exceptional behavior of square-like sites. However, that these sites display exceptional adsorption properties is a necessary though not sufficient condition for an extraordinary catalytic activity. This is why Figure 4a, for the particular case of the ORR on Au, contains a volcano plot in which it is possible to observe the effect on catalytic activities caused by deviations from trends in adsorption energies. The large deviations of (100) terraces are responsible for their selectivity toward the 4-electron pathway over the 2-electron pathway, as the location of the adsorption energies with respect to the equilibrium potentials ultimately determines the catalytic activity and selectivity.

The existence of the ensemble effect described here has another deep implication for (electro)catalysis: it causes the breaking of scaling relations[21,22,42,43] between the surface energetics of adsorbed intermediates, as shown in Figure 5 (see Figures S5, S6 and S14 for further details).

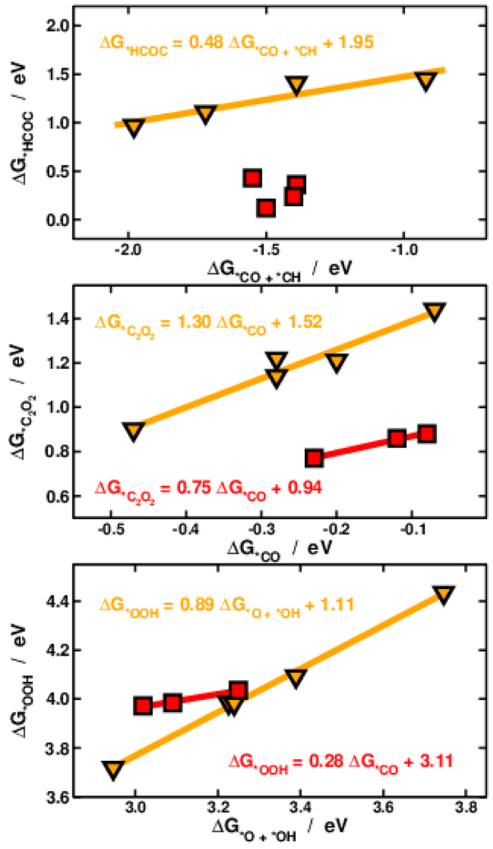

Figure 5. Scaling relations between the adsorption energies of *CO + *CH and *HCOC on Pt (top), *CO and $*C_2O_2$ on Cu (middle), and *O + *OH and *OOH on Au (bottom). In all cases, the hexagonal-symmetry sites (orange triangles) follow the expected linear trend, whereas the ensemble-effect sites (red squares) deviate from such trend.

The state-of-the-art design of new catalysts is based on linear scaling relations.[44] When these hold between the adsorbates involved in catalytic reactions, the degrees of freedom are reduced, thereby facilitating the modeling of complicated reactions through Sabatier-type activity plots. It is currently accepted that although scaling relations simplify catalytic reaction modeling, they also impose thermodynamic restrictions that are deleterious for the performance of heterogeneous catalysts and cause e.g., overpotentials.[42,43] Figure 5 indicates that structure sensitivity offers an excellent option for escaping scaling relations through ensemble effects. This allows, in turn, for further improvement of catalysts beyond the thermodynamic limits imposed by such relations.

4. CONCLUSION

Summarizing, this paper has identified the ensemble site for bond making and bond breaking on (100) surfaces as a site consisting of two opposing bridge sites, i.e., a double-bridge ensemble site, based on extensive density functional theory calculations of the mechanisms of dimethyl ether oxidation on platinum, carbon monoxide reduction on copper, ammonia oxidation on platinum, and oxygen reduction on gold. The existence of this site explains why these reactions all prefer the (100) terrace, and why steps and defects in the (100) surface lower the activity. The present work gives the fundamental understanding for an unusual particular type of structure sensitivity in heterogeneous (electro)catalysis involving the making or breaking of bonds between carbon, nitrogen and/or oxygen. Such unusual structure sensitivity is responsible for significant deviations in well-known scaling laws, which opens up the pathway for the design of superior heterogeneous catalysts.

■ ASSOCIATED CONTENT

Ⓢ Supporting Information

Supporting tables and figures. This material is available free of charge via the Internet at http://pubs.acs.org.

■ AUTHOR INFORMATION

Corresponding Authors

m.koper@chem.leidenuniv.nl
federico.calle-vallejo@ens-lyon.fr

Notes

The authors declare no competing financial interest.

■ ACKNOWLEDGMENTS

This work was supported by the Chinese Scholarship Council (CSC) through a CSC Scholarship awarded to H.L., The Netherlands Organization for Scientific Research (NWO), and the National Research School Combination Catalysis (NRSC-C, The Netherlands). The Stichting Nationale Computerfaciliteiten (National Computing Facilities Foundation, NCF) is gratefully acknowledged for the use of their supercomputer facilities, with financial support from NWO. Y. L. thanks the National 2011 Program of China via the Tianjin Co-innovative Research Center of Chemical Science and Engineering and the Natural Science Foundation of China under contract number 21120102039. F.C.V. acknowledges EU funding through the PUMA MIND contract (Call FCH-JU-2011-1, Code SP1-JTI-FCH-2011.1.3, Project 303419).

REFERENCES

(1) Somorjai, G. A.; Li, Y. *Introduction to Surface Chemistry and Catalysis*, 2nd ed.; Wiley: Hoboken NJ, 2010.
(2) Koper, M. T. M. *Nanoscale* **2011**, *3*, 2054.
(3) Vidal-Iglesias, F. J.; García-Aráez, N.; Montiel, V.; Feliu, J. M.; Aldaz, A. *Electrochem. Commun.* **2003**, *5*, 22.
(4) Vidal-Iglesias, F. J.; Solla-Gullón, J.; Montiel, V.; Feliu, J. M.; Aldaz, A. *J. Phys. Chem. B* **2005**, *109*, 12914.
(5) Li, H.; Calle-Vallejo, F.; Kolb, M. J.; Kwon, Y.; Li, Y.; Koper, M. T. M. *J. Am. Chem. Soc.* **2013**, *135*, 14329.
(6) Lu, L.; Yin, G.; Tong, Y.; Zhang, Y.; Gao, Y.; Osawa, M.; Ye, S. *J. Electroanal. Chem.* **2010**, *642*, 82.
(7) Tong, Y.; Lu, L.; Zhang, Y.; Gao, Y.; Yin, G.; Osawa, M.; Ye, S. *J. Phys. Chem. C* **2007**, *111*, 18836.
(8) Duca, M.; Figueiredo, M. C.; Climent, V.; Rodriguez, P.; Feliu, J. M.; Koper, M. T. M. *J. Am. Chem. Soc.* **2011**, *133*, 10928.
(9) Schouten, K. J. P.; Pérez Gallent, E.; Koper, M. T. M. *ACS Catal.* **2013**, *3*, 1292.
(10) Schouten, K. J. P.; Qin, Z.; Gallent, E. P.; Koper, M. T. M. *J. Am. Chem. Soc.* **2012**, *134*, 9864.
(11) Štrbac, S.; Adžić, R. R. *J. Electroanal. Chem.* **1996**, *403*, 169.
(12) Adić, R. R.; Marković, N. M.; Vešović, V. B. *J. Electroanal. Chem. Interfacial Electrochem.* **1984**, *165*, 105.
(13) Adžić, R. R.; Strbac, S.; Anastasijević, N. *Mater. Chem. Phys.* **1989**, *22*, 349.
(14) Weststrate, C. J.; Bakker, J. W.; Rienks, E. D. L.; Vinod, C. P.; Matveev, A. V.; Gorodetskii, V. V.; Nieuwenhuys, B. E. *J. Catal.* **2006**, *242*, 184.
(15) Vidal-Iglesias, F. J.; Solla-Gullón, J.; Rodríguez, P.; Herrero, E.; Montiel, V.; Feliu, J. M.; Aldaz, A. *Electrochem. Commun.* **2004**, *6*, 1080.
(16) Duca, M.; Rodriguez, P.; Yanson, A.; Koper, M. M. *Top. Catal.* **2014**, *57*, 255.
(17) Lu, L.; Yin, G.; Wang, Z.; Gao, Y. *Electrochem. Commun.* **2009**, *11*, 1596.
(18) Calle-Vallejo, F.; Martínez, J. I.; García-Lastra, J. M.; Sautet, P.; Loffreda, D. *Angew. Chem., Int. Ed.* **2014**, *53*, 8316.
(19) Heine, V.; Robertson, I. J.; Payne, M. C.; Murrell, J. N.; Phillips, J. C.; Weaire, D. *Philos. Trans. R. Soc., A* **1991**, *334*, 393.
(20) Robertson, I. J.; Payne, M. C.; Heine, V. *Europhys. Lett.* **1991**, *15*, 301.
(21) Abild-Pedersen, F.; Greeley, J.; Studt, F.; Rossmeisl, J.; Munter, T. R.; Moses, P. G.; Skúlason, E.; Bligaard, T.; Nørskov, J. K. *Phys. Rev. Lett.* **2007**, *99*, 016105.
(22) Calle-Vallejo, F.; Martinez, J. I.; Garcia-Lastra, J. M.; Rossmeisl, J.; Koper, M. T. M. *Phys. Rev. Lett.* **2012**, *108*, 116103.
(23) Hori, Y.; Kikuchi, K.; Murata, A.; Suzuki, S. *Chem. Lett.* **1986**, 897.
(24) Hori, Y.; Kikuchi, K.; Suzuki, S. *Chem. Lett.* **1985**, 1695.
(25) Calle-Vallejo, F.; Koper, M. T. M. *Angew. Chem., Int. Ed.* **2013**, *52*, 7282.
(26) Gattrell, M.; Gupta, N.; Co, A. *J. Electroanal. Chem.* **2006**, *594*, 1.
(27) Uribe, F. A.; Sharp, P. R.; Bard, A. J. *J. Electroanal. Chem.* **1983**, *152*, 173.
(28) Hori, Y.; Takahashi, R.; Yoshinami, Y.; Murata, A. *J. Phys. Chem. B* **1997**, *101*, 7075.
(29) Tang, W.; Sanville, E.; Henkelman, G. *J. Phys.: Condens. Matter* **2009**, *21*, 084204.
(30) Rosca, V.; Duca, M.; de Groot, M. T.; Koper, M. T. M. *Chem. Rev.* **2009**, *109*, 2209.
(31) Rosca, V.; Koper, M. T. M. *Phys. Chem. Chem. Phys.* **2006**, *8*, 2513.
(32) Skachkov, D.; Venkateswara Rao, C.; Ishikawa, Y. *J. Phys. Chem. C* **2013**, *117*, 25451.
(33) Novell-Leruth, G.; Valcárcel, A.; Clotet, A.; Ricart, J. M.; Pérez-Ramírez, J. *J. Phys. Chem. B* **2005**, *109*, 18061.
(34) Koper, M. T. M. *Chem. Sci.* **2013**, *4*, 2710.
(35) Viswanathan, V.; Hansen, H. A.; Rossmeisl, J.; Nørskov, J. K. *ACS Catal.* **2012**, *2*, 1654.
(36) Norskov, J. K.; Rossmeisl, J.; Logadottir, A.; Lindqvist, L.; Kitchin, J. R.; Bligaard, T.; Jonsson, H. *J. Phys. Chem. B* **2004**, *108*, 17886.
(37) Casalongue, H. S.; Kaya, S.; Viswanathan, V.; Miller, D. J.; Friebel, D.; Hansen, H. A.; Nørskov, J. K.; Nilsson, A.; Ogasawara, H. *Nat. Commun.* **2013**, *4*, 2817.
(38) Štrbac, S.; Adžić, R. R. *J. Electroanal. Chem.* **1992**, *337*, 355.
(39) Bligaard, T.; Nørskov, J. K.; Dahl, S.; Matthiesen, J.; Christensen, C. H.; Sehested, J. *J. Catal.* **2004**, *224*, 206.
(40) Norskov, J. K.; Bligaard, T.; Hvolbaek, B.; Abild-Pedersen, F.; Chorkendorff, I.; Christensen, C. H. *Chem. Soc. Rev.* **2008**, *37*, 2163.
(41) Van Santen, R. A. *Acc. Chem. Res.* **2008**, *42*, 57.
(42) Koper, M. T. M. *J. Electroanal. Chem.* **2011**, *660*, 254.
(43) Man, I. C.; Su, H.-Y.; Calle-Vallejo, F.; Hansen, H. A.; Martinez, J. I.; Inoglu, N. G.; Kitchin, J.; Jaramillo, T. F.; Norskov, J. K.; Rossmeisl, J. *ChemCatChem.* **2011**, *3*, 1159.
(44) Norskov, J. K.; Bligaard, T.; Rossmeisl, J.; Christensen, C. H. *Nat. Chem.* **2009**, *1*, 37.